

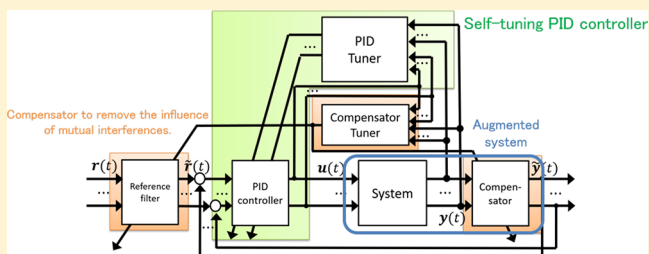
Design of an Augmented Output-Based Multiloop Self-Tuning PID Control System

Yoichiro Ashida, Shin Wakitani, and Toru Yamamoto*^{ID}

Graduate School of Engineering, Hiroshima University, Higashi-Hiroshima City 739-8527, Japan

ABSTRACT: Since the control performance of a proportional–integral–derivative (PID) control systems strongly depends on PID gains, lots of schemes for tuning PID gains have been proposed up to now. Recently, data-driven PID tuning schemes whose PID gains are directly determined from the closed-loop operating data attract attention. Lots of controlled objects are multi-input/multi-output systems, though almost data-driven PID tuning schemes target single-input/single-output systems. In this paper, a new design method of a multiloop self-tuning PID controller is proposed.

The proposed scheme first employs a postdecoupler to remove the influence of mutual interference. The multiloop self-tuning PID controller is designed for the approximately decoupled system. The effectiveness of the control scheme is evaluated by numerical and experimental examples.



■ INTRODUCTION

In the past decade, some data-driven (model-free) design methods have been proposed to determine control parameters.^{1–4} The data-driven tuning methods determine control parameters directly from operating data. In other words, system models are not used to design the controller in the data-driven methods. They attract attention as an effective method for process systems since it is difficult to accurately identify controlled objects. Nevertheless, identifying a system model is important because the model has much information about the system. Therefore, it is considered that an interplay of model-based and data-driven approaches are also very important. However, proportional–integral–derivative (PID) controllers have been widely employed in process industries.^{5–7} The authors have also proposed a data-driven PID control method⁸ and a data-driven self-tuning PID control method.⁹ Most of them are for single-input/single-output (SISO) systems. However, many process systems are multi-input/multi-output (MIMO) with mutual interference. In many cases, the interference is often neglected and a multiloop PID control system is constructed. However, sometimes desired control performance cannot be obtained. A data-driven PID controller design method for MIMO systems¹⁰ has also been proposed. However, p^2 PID controllers are required for p -input/ p -output systems, which not only make implementation difficult but also make it difficult to understand the physical meanings of PID gains. Some decoupling control schemes^{11–14} have been proposed for MIMO systems. The decoupler reduces the influence of interference from the augmented system consisting of the controlled object and the decoupler. A predecoupler is often designed on the basis of an inverse Nyquist array.^{15,16} However, if there is saturation at the input, the saturation is included inside the augmented system and the influence of interference is not effectively eliminated.

Some data-driven multivariable control schemes have been proposed.^{17–19} In addition, many model-based or data-driven sophisticated approaches that have already applied in actual systems have been proposed.^{20–23} Some of them can control a nonlinear system, and stability is analyzed under some conditions. However, most of the schemes are not for PID controllers or multiloop controllers. Therefore, the motivation of this research is to develop a decoupling self-tuning PID control scheme based on a data-driven PID control method.

In this paper, a design method of the augmented output-based multiloop self-tuning PID control system is proposed. A decoupling control is realized by using a decoupler provided by a static gain matrix in the proposed method. A feature of the proposed method is that the decoupler is designed as a postdecoupler. By use of the postdecoupler, the saturation is not included in the augmented system. In addition, a self-tuning PID control system⁹ is designed for an augmented system for the purpose of improving the performance of the multiloop PID control system. A self-tuning PID control is one of the self-tuning control algorithms, and the controller structure is limited to the PID controller. Moreover, in order to design the adaptive control system, a recursive algorithm for identifying a static gain matrix is introduced. The proposed method uses a simple system model and data-driven PID control scheme. Thus, the main contribution of this work is to suggest a decoupling PID control scheme with an interplay of data-driven and model-based approaches. This paper is organized as follows. In the first

section, we provide a description of MIMO systems. In the second section, we describe the design of a decoupler that performs decoupling and the design method for a self-tuning PID control system for multiloop PID control. In the third section, the effectiveness of the proposed control method is numerically verified, and behavior of the proposed control method is experimentally examined by employing to a pilot-scale plant in the fourth section.

■ SYSTEM DESCRIPTION

In this paper, scalars, vectors, and matrices are expressed by a lower case with italic font, a lower case with a bold italic font and a capital letter with a bold italic font except transfer functions. Transfer functions and transfer function matrices are expressed by a capital letter with italic and a capital letter with bold italic. Consider the p -input/ p -output multivariable discrete-time system given by the following equation:

$$\mathbf{A}(z^{-1}) \mathbf{y}(k) = \mathbf{D}(z^{-1}) \mathbf{B}(z^{-1}) \mathbf{u}(k-1) \quad (1)$$

where z^{-1} is a shift operator such that $z^{-1}y(k) = y(k-1)$. $\mathbf{y}(k)$ and $\mathbf{u}(k)$ are the p -dimensional control output vector and control input vector as expressed by the following equations:

$$\mathbf{y}(k) = [y_1(k), y_2(k), \dots, y_p(k)]^T \quad (2)$$

$$\mathbf{u}(k) = [u_1(k), u_2(k), \dots, u_p(k)]^T \quad (3)$$

where $i = 1, 2, \dots, p$, and in the following, i is thus given unless otherwise stated. Furthermore, $\mathbf{A}(z^{-1})$ and $\mathbf{B}(z^{-1})$ are the following polynomial matrices:

$$\mathbf{A}(z^{-1}) = \text{diag}\{A_1(z^{-1}), A_2(z^{-1}), \dots, A_p(z^{-1})\} \quad (4)$$

$$A_i(z^{-1}) = 1 + a_{i,1}z^{-1} + a_{i,2}z^{-2} + \dots + a_{i,n}z^{-n} \quad (5)$$

$$\mathbf{B}(z^{-1}) = \begin{bmatrix} B_{1,1}(z^{-1}) & B_{1,2}(z^{-1}) & \dots & B_{1,p}(z^{-1}) \\ B_{2,1}(z^{-1}) & B_{2,2}(z^{-1}) & \dots & B_{2,p}(z^{-1}) \\ \vdots & \vdots & \ddots & \vdots \\ B_{p,1}(z^{-1}) & B_{p,2}(z^{-1}) & \dots & B_{p,p}(z^{-1}) \end{bmatrix} \quad (6)$$

$$= \mathbf{B}_0 + \mathbf{B}_1 z^{-1} + \dots + \mathbf{B}_m z^{-m} \quad (7)$$

n and m represent the orders of $\mathbf{A}(z^{-1})$ and $\mathbf{B}(z^{-1})$, respectively. \mathbf{B}_j ($j = 1, 2, \dots, m$) is as follows:

$$\mathbf{B}_j = \begin{bmatrix} b_{j,1,1} & b_{j,1,2} & \dots & b_{j,1,p} \\ b_{j,2,1} & b_{j,2,2} & \dots & b_{j,2,p} \\ \vdots & \vdots & \ddots & \vdots \\ b_{j,p,1} & b_{j,p,2} & \dots & b_{j,p,p} \end{bmatrix} \quad (8)$$

$\mathbf{D}(z^{-1})$ is a matrix representing time delay and is a diagonal matrix as follows:

$$\mathbf{D}(z^{-1}) = \text{diag}\{z^{-d_1}, z^{-d_2}, \dots, z^{-d_p}\} \quad (9)$$

In this paper, the controlled object satisfies the following assumptions.

1. The polynomial matrices $\mathbf{A}(z^{-1})$ and $\mathbf{B}(z^{-1})$ are asymptotically stable.
2. $\det \mathbf{B}(1) \neq 0$.

■ AUGMENTED OUTPUT-BASED MULTILOOP SELF-TUNING PID CONTROL SYSTEM

Figure 1 presents a block diagram of the multiloop self-tuning PID control system proposed in this paper. The reference signal

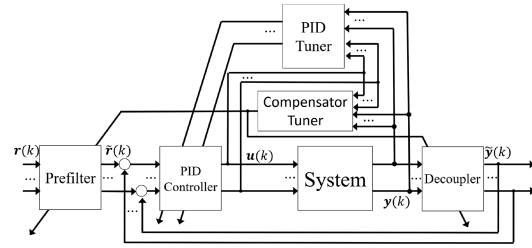


Figure 1. Schematic diagram of the proposed control scheme.

$r(k)$, the filtered output $\tilde{r}(k)$, and the output of the augmented system $\tilde{y}(k)$ are p -dimensional vectors expressed by the following equation:

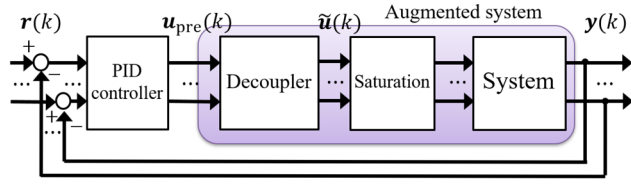
$$\mathbf{r}(k) = [r_1(k), r_2(k), \dots, r_p(k)]^T \quad (10)$$

$$\tilde{\mathbf{r}}(k) = [\tilde{r}_1(k), \tilde{r}_2(k), \dots, \tilde{r}_p(k)]^T \quad (11)$$

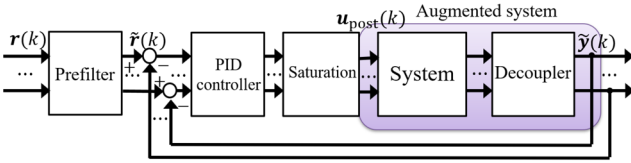
$$\tilde{\mathbf{y}}(k) = [\tilde{y}_1(k), \tilde{y}_2(k), \dots, \tilde{y}_p(k)]^T \quad (12)$$

where it is assumed that the reference signal is given a piecewise constant. The purpose of the control is to regulate the controlled outputs to the reference set point. In addition, a reference model is introduced to realize desired response. Therefore, the proposed method intends to make controlled outputs track reference models defined by operators. The proposed method shown in Figure 1 can be divided into two sections. The first section includes decoupler, decoupler tuner, and prefilter. The section makes an augmented system constructed with a system and decoupler. The augmented can be divided into two parts. The first part makes an augmented system constructed with a system and decoupler. The part includes decoupler, decoupler tuner, and prefilter. The augmented system can be approximately regarded as a system without interference. The second part is a controller part and controls the augmented system. The part includes a PID controller and a PID tuner and can be regarded as a system without interference. Why the postdecoupler is employed in the proposed method is explained below. The closed-loop systems using predecoupler and postdecoupler are shown in Figure 2. In the upper-side figure, $\mathbf{u}_{\text{pre}}(k)$ and $\mathbf{y}(k)$ are used for determining PID gains. In the lower-side figure, $\mathbf{u}_{\text{post}}(k)$ and $\tilde{\mathbf{y}}(k)$ are also used. In many cases, $\mathbf{u}_{\text{post}}(k)$ can be obtained because a saturation function is in a computer like DCS. When the predecoupler is employed, it is clear that the relationship between $\mathbf{u}_{\text{pre}}(k)$ and $\mathbf{y}(k)$ is nonlinear because the augmented system contains a saturation. In contrast, the relation of the $\mathbf{u}_{\text{post}}(k)$ and $\tilde{\mathbf{y}}(k)$ of the closed-loop using a postdecoupler is linear because a saturation exists before the augmented system. Therefore, the saturation may cause the wrong effect in tuning PID gain affects the PID gain tuning.

Design of the Postdecoupler. An important issue in designing a multiloop control system for a MIMO system is how to eliminate, or at least reduce, the influence of mutual interference. In this paper, decoupling by inserting a postdecoupler for the controlled object is introduced. As a result, the augmented system composed of the controlled object and postdecoupler is treated as a set of SISO systems. In



(a) Block diagrams using pre-decoupler



(b) Block diagram using post-decoupler, and the proposed method employs this type of a decoupler

Figure 2. Block diagrams of closed-loops using predecoupler and postdecoupler

controlling a MIMO process system with a relatively slow response, a static decoupler based on a gain matrix is often used as a decoupler. This is due to the following reasons:

1. In process control systems, control that focuses more on low-frequency components than high frequency components is required.
2. It is difficult to identify a high order system accurately due to the influence noise.

For the above reasons, we also use the following static decoupler in this paper.

The following matrix is employed as a decoupler:

$$\mathbf{H} = \mathbf{B}^{-1}(1) \mathbf{A}(1) = \begin{bmatrix} H_{1,1} & H_{1,2} & \cdots & H_{1,p} \\ H_{2,1} & H_{2,2} & \cdots & H_{2,p} \\ \vdots & \vdots & \ddots & \vdots \\ H_{p,1} & H_{p,2} & \cdots & H_{p,p} \end{bmatrix} \quad (13)$$

This is the inverse matrix of static gains, and the gain matrix of the augmented system becomes a unit matrix as a result of this decoupler, with static decoupling achieved. However, since $\tilde{y}(k) \neq y(k)$ in Figure 1, even if $\tilde{y}(k)$ follows $r(k)$, $y(k)$ does not follow $r(k)$. In order to deal with this problem, a prefilter is introduced. The values in the steady state of the control output vector, reference vector, prefilter output vector, and augmented output vector shown in eqs 2 and 10–12 are respectively \bar{y} , \bar{r} , \bar{r} , and \bar{y} . When the augmented output \bar{y} is the same as the filtered output \bar{r} in the steady state, the following relationship holds:

$$\bar{y} = \bar{r} = \mathbf{B}^{-1}(1) \mathbf{A}(1) \bar{y} \quad (14)$$

Therefore, when assigning \bar{r} as follows, it is possible to make the control output \bar{y} follow the reference signal \bar{r} .

$$\bar{r} = \mathbf{B}^{-1}(1) \mathbf{A}(1) \bar{r} \quad (15)$$

From eq 15, the prefilter must be as follows:

$$\mathbf{H}_{\text{ref}} = \mathbf{B}^{-1}(1) \mathbf{A}(1) \quad (16)$$

That is, the same matrix as the postdecoupler may be used as the prefilter. By using the postdecoupler and the prefilter, it is possible to statically decouple the controlled object and use the design method for a SISO control system.

Design of the Self-Tuning PID Controller. By use of a decoupler described in a previous section, the augmented system can be approximately regarded as a p-input/p-output system without interference. Therefore, some control schemes for a SISO system can be employed to control the augmented system. Many methods have been proposed for designing multiloop PID control systems. In this paper, we aim to reduce the cost of implementation and effectively utilizing existing PID controllers. The following discrete-time PID controller is employed:

$$\Delta u_i(k) = K_{I_i} \{ \tilde{r}_i(k) - \tilde{y}_i(k) \} - K_{P_i} \Delta \tilde{y}_i(k) - K_{D_i} \Delta^2 \tilde{y}_i(k) \quad (17)$$

where Δ is a differencing operator represented by $\Delta := 1 - z^{-1}$. The suffix i indicates that it is the physical quantity of the i th control loop. K_{P_i} , K_{I_i} , and K_{D_i} are proportional gain, integral gain, and differential gain, respectively. By transforming eq 17, the following equation can be obtained.

$$\begin{aligned} \frac{1}{K_{I_i}} \Delta u_i(k) + \frac{K_{P_i} + K_{I_i} + K_{D_i}}{K_{I_i}} \tilde{y}_i(k) - \frac{K_{P_i} + 2K_{D_i}}{K_{I_i}} \tilde{y}_i(k-1) \\ + \frac{K_{D_i}}{K_{I_i}} \tilde{y}_i(k-2) - \tilde{r}_i(k) = 0 \end{aligned} \quad (18)$$

The augmented output $\phi_i(k)$ is defined as follows:

$$\begin{aligned} \phi_i(k) := \hat{a}_1(k) \Delta u_i(k) + \hat{a}_2(k) \{ \tilde{y}_i(k) - \tilde{y}_i(k-2) \} \\ + \hat{a}_3(k) \{ \tilde{y}_i(k-1) - \tilde{y}_i(k-2) \} + \tilde{y}_i(k-2) \end{aligned} \quad (19)$$

where each coefficient is expressed by the following equation:

$$\left. \begin{aligned} a_1 &:= \frac{1}{K_{I_i}} \\ a_2 &:= \frac{K_{P_i} + K_{I_i} + K_{D_i}}{K_{I_i}} \\ a_3 &:= -\frac{K_{P_i} + 2K_{D_i}}{K_{I_i}} \end{aligned} \right\} \quad (20)$$

From eqs 18–20, the following relationship can be obtained:

$$\phi_i(k) = \tilde{r}_i(k) \quad (21)$$

The purpose of control is to make the system output $\tilde{y}_i(k)$ follow the output $\tilde{y}_{m_i}(k)$ of the desired reference model $G_{m_i}(z^{-1})$. The reference model is designed as follows:

$$G_{m_i}(z^{-1}) := \frac{z^{-(d_i+1)} P_{m_i}(1)}{P_{m_i}(z^{-1})} \quad (22)$$

$$P_{m_i}(z^{-1}) = 1 + p_1 z^{-1} + p_2 z^{-2} \quad (23)$$

where p_1 and p_2 are determined by the following equations:

$$\left. \begin{aligned} p_{1_i} &= -2 \exp\left(-\frac{\rho_i}{2\mu_i}\right) \cos\left(\frac{\sqrt{4\mu_i - 1}}{2\mu_i} \rho_i\right) \\ p_{2_i} &= \exp\left(-\frac{\rho_i}{\mu_i}\right) \\ \rho_i &:= T_s/\sigma_i \\ \mu_i &:= 0.25(1 - \delta_i) + 0.51\delta_i \end{aligned} \right\} \quad (24)$$

σ_i and μ_i are related to the rise time and the damping coefficient, respectively, and are user-specified parameters. Refer to refs 9 and 11 for the details of a design method of the reference model.

$$\tilde{y}_{m_i}(k) = G_{m_i}(z^{-1}) \tilde{y}_i(k) \quad (25)$$

Next, the cost function J_i is defined as follows:

$$J_i = \sum_{j=1}^{N_i} \varepsilon_i(j)^2 \quad (26)$$

where N_i is the total number of data and the augmented error $\varepsilon_i(k)$ is defined as follows:

$$\varepsilon_i(k) = G_{m_i}(z^{-1}) \phi_i(k) - \tilde{y}_i(k) \quad (27)$$

By minimization of the cost function J_i , the following optimization is performed:

$$G_{m_i}(z^{-1}) \phi_i(k) \rightarrow \tilde{y}_i(k) \quad (28)$$

$a_j (j = 1, 2, 3)$ included in (19) is computed by the optimization. That is, if sufficient optimization is carried out, the following relation can be obtained:

$$G_{m_i}(z^{-1}) \phi_i(k) = \tilde{y}_i(k) \quad (29)$$

In Figure 3, the inputs of the block diagrams are the same as in eq 21. In addition, the output of the block diagrams is also the same

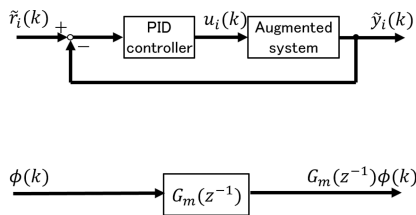


Figure 3. Schematic diagram of the PID tuning scheme.

as in eq 29. Therefore, by designing the controller using the optimized a_j , the closed-loop transfer function is identical to the reference model. PID gains are calculated from a_j by the following equations:

$$\left. \begin{aligned} K_{P_i} &= \frac{2\hat{a}_{2_i} + \hat{a}_{3_i} - 2}{\hat{a}_{1_i}} \\ K_{I_i} &= \frac{1}{\hat{a}_{1_i}} \\ K_{D_i} &= \frac{1 - \hat{a}_{2_i} - \hat{a}_{3_i}}{\hat{a}_{1_i}} \end{aligned} \right\} \quad (30)$$

where \hat{a}_j denotes the estimated value corresponding to a_j .

Design of the Self-Tuning PID Control System. The design method discussed above is extended to the self-tuning PID control method. First, in order to design the decoupler, the system gain matrix is required. The system parameters included in eq 1 are estimated by the following recursive least-squares (RLS) method.²⁴

$$\hat{\theta}_{1,i}(k) = \hat{\theta}_{1,i}(k-1) - \mathbf{K}_{1,i}(k) y_{f_i}(k) \quad (31)$$

$$\mathbf{K}_{1,i}(k) = \frac{\mathbf{P}_{1,i}(k-1) \boldsymbol{\varphi}_{1,i}(k-1)}{\omega_{1,i} + \boldsymbol{\varphi}_{1,i}^T(k-1) \mathbf{P}_{1,i}(k-1) \boldsymbol{\varphi}_{1,i}(k-1)} \quad (32)$$

$$\mathbf{P}_{1,i}(k) = \frac{1}{\omega_{1,i}} \left[\mathbf{P}_{1,i}(k-1) - \frac{\mathbf{P}_{1,i}(k-1) \boldsymbol{\varphi}_{1,i}(k-1) \boldsymbol{\varphi}_{1,i}^T(k-1) \mathbf{P}_{1,i}(k-1)}{\omega_{1,i} + \boldsymbol{\varphi}_{1,i}^T(k-1) \mathbf{P}_{1,i}(k-1) \boldsymbol{\varphi}_{1,i}(k-1)} \right] \quad (33)$$

$\omega_{1,i}$ are forgetting factors, and $\hat{\theta}_{1,i}(k)$ and $\boldsymbol{\varphi}_{1,i}(k)$ are as follows:

$$\hat{\theta}_{1,i}(k) := [a_{i,1}(k), \dots, a_{i,n}(k), b_{0,i,1}(k), \dots, b_{m,i,1}(k), \dots, b_{0,i,p}(k), \dots, b_{m,i,p}(k)]^T \quad (34)$$

$$\boldsymbol{\varphi}_{1,i}(k) := [y_{f_i}(k-1), \dots, y_{f_i}(k-n), u_{f_i}(k-d_1-1), \dots, u_{f_i}(k-d_1-m), u_{f_i}(k-d_p-1), \dots, u_{f_i}(k-d_p-m)]^T \quad (35)$$

The initial estimate $\hat{\theta}_{1,i}(0)$, the initial covariance matrix $\mathbf{P}_{1,i}(0)$, and forgetting factor $\omega_{1,i}$ are user-specified parameters. In addition, orders of transfer functions m and n , and estimated delay time $d_i (i = 1, 2, \dots, p)$ are also user-specified parameters. $\omega_{1,i}$ is often set between 0.98 and 1. If delay time and orders are known, m , n , and d_i are easily determined. If they are unknown, d_i should be set as a minimum number of estimated delay time or zero, and m and n should be set as large enough numbers than true orders of a controlled object. $\hat{\theta}_{1,i}(0)$ is given by

$$\hat{\theta}_{1,i}(0) = [\hat{a}_{i,1}(0), \dots, \hat{a}_{i,n}(0), \hat{b}_{0,i,1}(0), \dots, \hat{b}_{m,i,1}(0), \dots, \hat{b}_{0,i,p}(0), \dots, \hat{b}_{m,i,p}(0)] \quad (36)$$

The value of $\hat{\theta}_{1,i}(0)$ does not affect control performance strongly. $\mathbf{P}_{1,i}(0)$ is often determined as follows:

$$\mathbf{P}_{1,i}(0) = \alpha_{1,i} \mathbf{I} \quad (37)$$

\mathbf{I} denotes the identity matrix, and $\alpha_{1,i}$ is also a user-specified parameter. $\alpha_{1,i}$ is often set between 1 and 1000. The postdecoupler is calculated by the static system gain. A low-pass filter $C_1(z^{-1})$ such as the following equation is employed to all input and output signals of the system so as to obtain a more accurate estimation result of the static gain:

$$C_1(z^{-1}) := \frac{1 - c_1}{1 - c_1 z^{-1}} \quad (38)$$

c_1 is a parameter for determining the cutoff frequency and should be set with considering noise strength. At this time, $y_{f_i}(k)$ and $u_{f_i}(k)$ in eqs 31 and 35 are as follows:

$$y_f(k) := C_1(z^{-1}) y_i(k) \quad (39)$$

$$u_f(k) := C_1(z^{-1}) u_i(k) \quad (40)$$

If the accurate time delay and the orders n and m are unknown in this system identification, the time delay should be set smaller than the expected value and the order should be taken as larger. The greater the number of estimation parameters, the less accurate individual estimates are due to noise. However, by calculating static gains in designing of the decoupler, the effect of noise is alleviated.

By use of eqs 31–40, the decoupler can be calculated. Next, the multiloop self-tuning PID controller is designed. That is, by use of the following RLS method, $\hat{a}_j(k)$ is computed in an online manner.

$$\hat{\theta}_{2,i}(k) = \hat{\theta}_{2,i}(k-1) - \mathbf{K}_{2,i}(k) y_f(k) \quad (41)$$

$$\mathbf{K}_{2,i}(k) = \frac{\mathbf{P}_{2,i}(k-1) \boldsymbol{\varphi}_{2,i}(k-1)}{\omega_{2,i} + \boldsymbol{\varphi}_{2,i}^T(k-1) \mathbf{P}_{2,i}(k-1) \boldsymbol{\varphi}_{2,i}(k-1)} \quad (42)$$

$$\mathbf{P}_{2,i}(k) = \frac{1}{\omega_{2,i}} \left[\mathbf{P}_{2,i}(k-1) - \frac{\mathbf{P}_{2,i}(k-1) \boldsymbol{\varphi}_{2,i}(k-1) \boldsymbol{\varphi}_{2,i}^T(k-1) \mathbf{P}_{2,i}(k-1)}{\omega_{2,i} + \boldsymbol{\varphi}_{2,i}^T(k-1) \mathbf{P}_{2,i}(k-1) \boldsymbol{\varphi}_{2,i}(k-1)} \right] \quad (43)$$

where $\omega_{2,i}$ is a forgetting factor, while $\hat{\theta}_{2,i}(k)$ and $\boldsymbol{\varphi}_{2,i}(k)$ are as follows:

$$\hat{\theta}_{2,i}(k) := [\hat{a}_1(k) \hat{a}_2(k) \hat{a}_3(k)]^T \quad (44)$$

$$\boldsymbol{\varphi}_{2,i}(k) := G_{m_i}(z^{-1}) \times [\Delta u_{g_i}(k), \tilde{y}_{g_i}(k) - \tilde{y}_{g_i}(k-2), \tilde{y}_{g_i}(k-1) - \tilde{y}_{g_i}(k-2)]^T \quad (45)$$

The initial estimate $\hat{\theta}_{2,i}(0)$, the initial covariance matrix $\mathbf{P}_{2,i}(0)$, and forgetting factors $\omega_{2,i}$ are user-specified parameters. $\hat{\theta}_{1,i}(0)$ is as follows:

$$\hat{\theta}_{1,i}(0) = [\hat{a}_1(0), \hat{a}_2(0), \hat{a}_3(0)] \quad (46)$$

$\mathbf{P}_{2,i}(0)$ is determined by the same as $\mathbf{P}_{1,i}(0)$, that is,

$$\mathbf{P}_{2,i}(0) = \alpha_{2,i} \mathbf{I} \quad (47)$$

$\tilde{y}_{g_i}(k)$ and $u_{g_i}(k)$ in eqs 41 and 45 are the filtered inputs and outputs of the augmented system as follows:

$$\tilde{y}_{g_i}(k) := C_2(z^{-1}) \tilde{y}_i(k) \quad (48)$$

$$u_{g_i}(k) := C_2(z^{-1}) u_i(k) \quad (49)$$

$C_2(z^{-1})$ is designed as follows:

$$C_2(z^{-1}) := \frac{1 - c_2}{1 - c_2 z^{-1}} \quad (50)$$

c_2 is a parameter for determining the cutoff frequency. User-specified parameters of the RLS algorithm should be set the same way as for the previous RLS method. The multiloop self-tuning PID control algorithm is summarized below.

1. Determine user-specified parameters shown as Table 1. Some consideration of the parameters are written after this outline.

Table 1. User-Specified Parameters

system parameters		PID gains	
n	order of transfer function	σ_i	rise time of reference model
m	order of transfer function	δ_i	damping-factor of reference model
d_p	delay-time of transfer function	d_i	delay-time
$\omega_{1,i}$	forgetting factor	$\omega_{2,i}$	forgetting factor
$\alpha_{1,i}$	initial value of covariance matrix	$\alpha_{2,i}$	initial value of covariance matrix
c_1	coefficient low-pass filter	c_2	coefficient low-pass filter
$\hat{\theta}_{1,i}(0)$	initial estimation vector	$\hat{\theta}_{2,i}(0)$	initial estimation vector

2. Calculate the filtered inputs $u_f(k)$ and outputs $y_f(k)$ for system identification by using eqs 39 and 40.
3. Identify $\hat{\theta}_{1,i}(k)$ by using the RLS method shown in eqs 31 to 37.
4. Compute transfer function matrix $A^{-1}(z^{-1}) D(z^{-1}) B(z^{-1})$ on the basis of the identified $\hat{\theta}_{1,i}(k)$.
5. Calculate a static system gain matrix by substituting $z^{-1} = 1$ to the transfer function matrix $A^{-1}(z^{-1}) D(z^{-1}) B(z^{-1})$.
6. Calculate the decoupler from the static gain matrix by using eq 13.
7. Compute the $\tilde{y}(k)$ from the controlled output and the decoupler by using $\tilde{y}(k) = \mathbf{H}y(k)$.
8. Calculate the filtered inputs $u_{g_i}(k)$ and outputs $\tilde{y}_{g_i}(k)$ by using eqs 48 and 49.
9. Calculate $\hat{\theta}_{2,i}(k)$ by using the RLS method shown in eqs 41–47.
10. Compute PID gains on the basis of the $\hat{a}_j(k)$ of $\hat{\theta}_{2,i}(k)$ by using eq 30.
11. The filtered reference signal $\tilde{r}(k)$ is calculated by using $\tilde{r}(k) = \mathbf{H}_{ref} r(k)$, and input signals are calculated.
12. Controlled output is obtained on the basis of the calculated input at 3.3.
13. Go to the first step as $k = k + 1$.

Some considerations for determining user-specified parameters are written as follows. If n , m , and d_p are unknown, d_p should be set as a minimum number of estimated delay time or zero, and m and n should be set as large enough numbers than true orders of a controlled object. σ_i should be determined corresponding to complexity of a system. If a controlled system has a long dead time and is high-order, σ_i should be large. δ_i is considered to be set as zero in many processes. If a dead time of the process is unknown, d_i should be larger than the true value because calculated PID gains become bigger when d_i is small. $\omega_{1,i}$ and $\omega_{2,i}$ are often set between 0.98 and 1. $\alpha_{1,i}$ and $\alpha_{2,i}$ are often set between 1 and 1000. c_1 and c_2 are not important if the system noise is small. If the noise is strong, c_1 and c_2 are determined to reduce the influence of noise. $\hat{\theta}_{1,i}(0)$ is considered to set as an estimated system model becomes stable. From $\hat{\theta}_{2,i}(0)$, initial PID gains are calculated, then $\hat{\theta}_{2,i}(0)$ should be set as initial PID gains are small.

At last, convergence and stability are mentioned. In the proposed method, the influence of interferences is not removed perfectly in the transient state because a decoupler is static. Therefore, it is difficult to prove the convergence and stability

precisely. From the viewpoint of the overall proposed method, richness conditions of the input signals are not required to determine the decoupler because the proposed method utilizes a static decoupler. As a result, approximately accurate decoupler can be identified easily. When the decoupler works effectively, the influence of the interference is small, and the control loop is less likely to be unstable. In addition, the stability can be improved to employ a sluggish reference model. Concretely speaking, the larger rise time σ_i can be used, and sometimes it is effective to set the dead time d_i larger.

■ SIMULATION

Time-Invariant System. The controlled object is given by the following equation:

$$\mathbf{G}(s) = \begin{bmatrix} \frac{7.3}{23s^2 + 83s + 1} e^{-25s} & \frac{-4.4}{14s^2 + 85s + 1} e^{-25s} \\ \frac{3.8}{19s^2 + 105s + 1} e^{-20s} & \frac{6.1}{18s^2 + 102s + 1} e^{-20s} \end{bmatrix} \quad (51)$$

The system is discretized by $T_s = 1$ s and the following discrete system can be obtained:

$$\begin{bmatrix} y_1(k) \\ y_2(k) \end{bmatrix} = \begin{bmatrix} \frac{0.06z^{-1} + 0.02z^{-2}}{1 - 1.02z^{-1} + 0.03z^{-2}} z^{-25} & \frac{-0.04z^{-1} - 0.008z^{-2}}{1 - 0.99z^{-1} + 0.002z^{-2}} z^{-25} \\ \frac{0.03z^{-1} + 0.006z^{-2}}{1 - 0.995z^{-1} + 0.004z^{-2}} z^{-20} & \frac{0.05z^{-1} + 0.01z^{-2}}{1 - 0.99z^{-1} + 0.003z^{-2}} z^{-20} \end{bmatrix} \times \begin{bmatrix} u_1(k) \\ u_2(k) \end{bmatrix} + \begin{bmatrix} \xi_1(k) \\ \xi_2(k) \end{bmatrix} \quad (52)$$

where $\xi_i(k)$ denotes the Gaussian white noise sequence with zero mean and variance 0.01^2 . The system has input saturation. The upper limit is set as 100 and the lower limit is set as 0. The step response of the controlled object is shown in Figure 4. It is clear that the system has the interference as the nondiagonal elements.

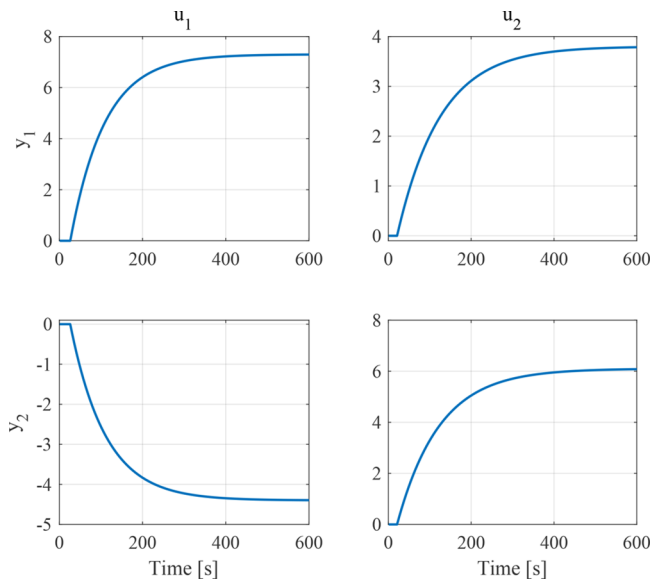


Figure 4. Step response of the controlled object.

The simulation result using the proposed method is described below. The description is associated with the algorithm outline shown at the end of the previous section. To apply the proposed method, user-specified parameters are set as shown in Table 2. This is the first step of the algorithm outline.

Table 2. User-Specified Parameters Corresponding to Figure 7

system parameters		PID gains	
n	10	σ_i	50
m	50	δ_i	0
d_p	0	d_i	known
$\omega_{1,i}$	1	$\omega_{2,i}$	0.995
$\alpha_{1,i}$	100	$\alpha_{2,i}$	100
c_1	0.95	c_2	0.5
$\hat{\theta}_{1,i}(0)$	unit vector	$\hat{\theta}_{2,i}(0)$	unit vector

Between the second and 13th of the outline is executed online. At the second to sixth steps, filtered inputs/outputs, static gain matrix, and a decoupler are calculated. By use of the recursive least-squares, a transfer function $\mathbf{A}^{-1}(z^{-1})\mathbf{D}(z^{-1})\mathbf{B}(z^{-1})$ is identified. From the transfer function, \mathbf{H} of eq 13 can be calculated. The calculation result of the static gain matrix is shown in Figure 5. It is clear that the estimated value converged to the true value.

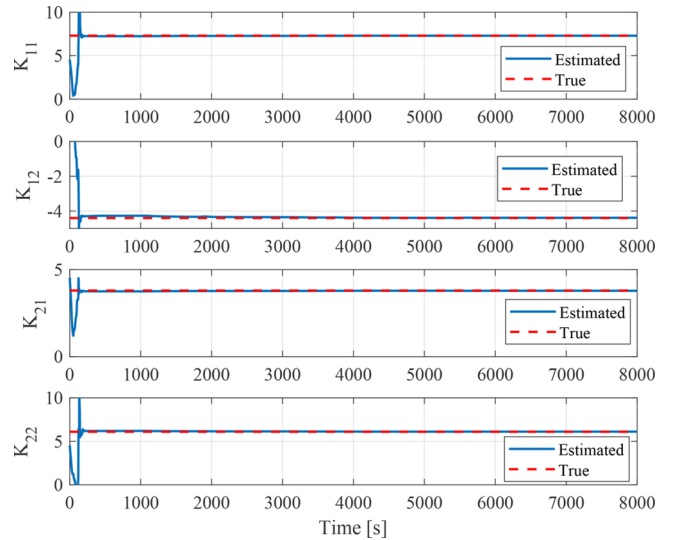


Figure 5. Trajectories of the system gain matrix corresponding to Figure 7.

Between the seventh and 10th steps, filtered inputs/outputs, $\hat{a}_p(k)$ and PID gains are calculated. By use of the RLS method, $\hat{a}_j(k)$ is calculated from the filtered inputs/outputs $u_g(k)$ and $\hat{y}_{g_i}(k)$. PID gains are determined on the basis of $\hat{a}_j(k)$ by using eq 30. The trajectories of the estimated PID gains are shown in Figure 6.

Next, filtered reference signals and controlled inputs are calculated. In addition, the controlled output is collected by using the calculated inputs. The control result of the proposed control scheme is shown in Figure 7. The good control result was obtained by the proposed method. Around 5500 steps, the control performance deteriorated. This is because the control

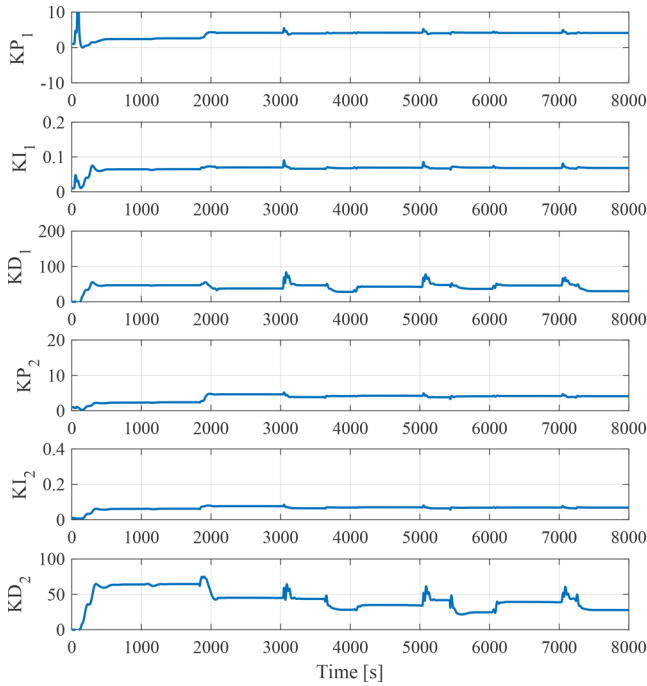


Figure 6. Trajectories of the PID gains corresponding to Figure 7.

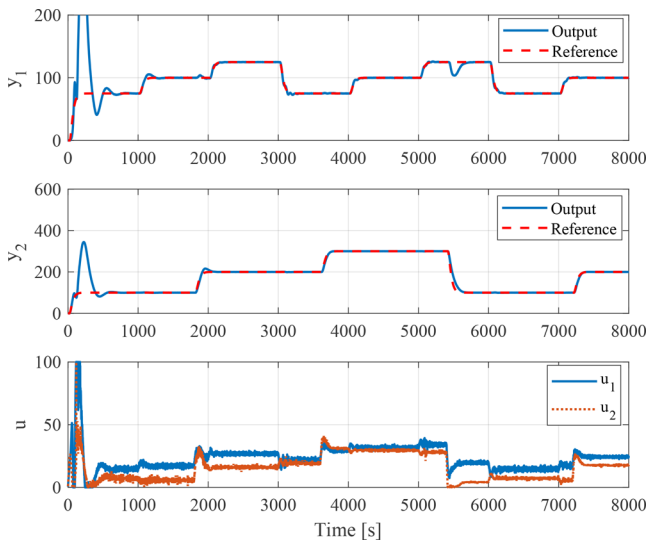


Figure 7. Control result for the time-invariant controlled object (eq 52) by using the proposed control method.

input was saturated. Thus, it was impossible to maintain the desired control performance.

The step response and the bode diagram of the augmented system are shown in Figure 8 and Figure 9, where the decoupler was designed by using the system gain matrix computed at final step of Figure 5. The step response shows that the nondiagonal elements are nearly zero. The bode diagram shows that gains of the nondiagonal elements become higher in the middle frequency. This means that the interferences of the transient state were not removed completely. In contrast, the diagonal elements are normal time-delay systems.

In the decoupling control, a predecoupler is often employed. However, as mentioned above, the predecoupler has a serious problem when the system has input saturation. In order to illustrate the problem, the self-tuning PID control method with a

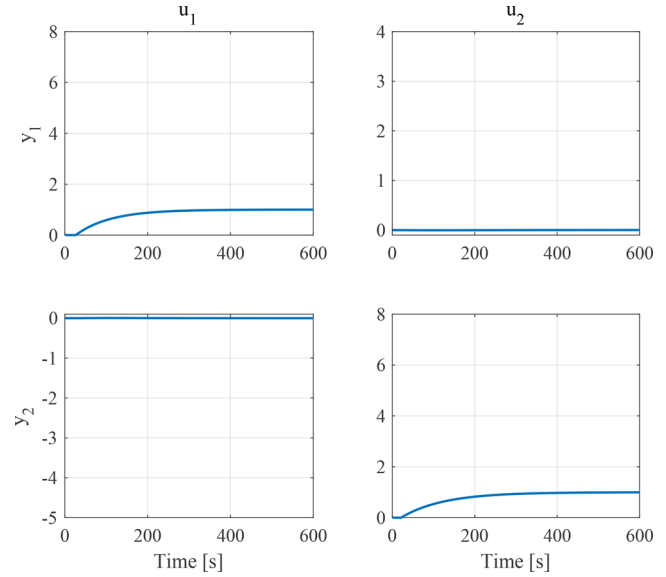


Figure 8. Step response of the augmented system of the time-invariant controlled object.

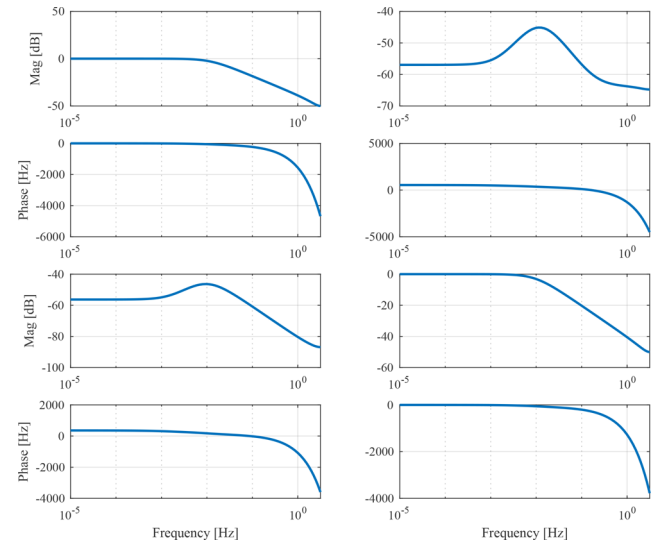


Figure 9. Bode diagram of the augmented system of the time-invariant controlled object.

predecoupler was employed. A control result using a predecoupler is shown in Figure 10. The trajectories of PID gains corresponding to Figure 10 are also shown in Figure 11. The user-specified parameters were set by the same as the proposed method. The control result got worse than the proposed method, as shown in Figure 10. Figure 11 shows the trajectories of PID gains corresponding to Figure 10. In comparison with Figures 7 and 10, the effectiveness of the postdecoupler is verified.

At last, a control result using a multivariable self-tuning PID controller¹¹ is shown to compare. The controller is designed on the basis of generalized minimum variance control (GMVC), and the design method is sometimes employed in industries. The control result is shown as Figure 12. User-specified parameters of the RLS algorithms and reference models are the same as the proposed method. There is an additional parameter λ in the GMVC-based tuning. When λ is set bigger, the control system becomes more stable. In this result, λ is set as

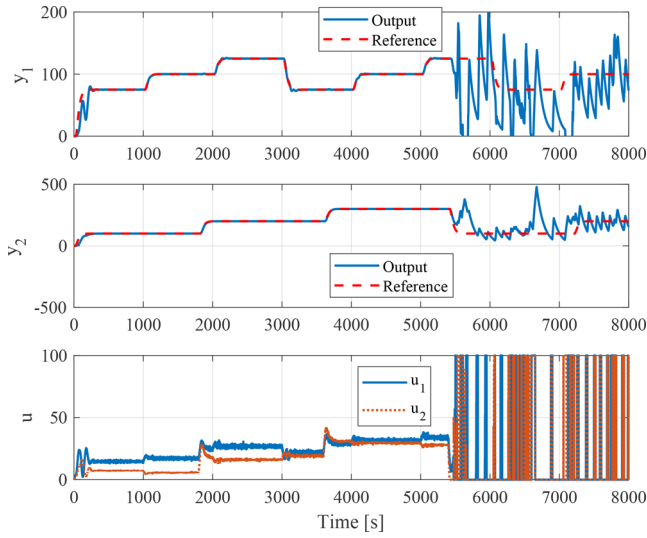


Figure 10. Control result of the time-invariant controlled object with delay using predecoupler.

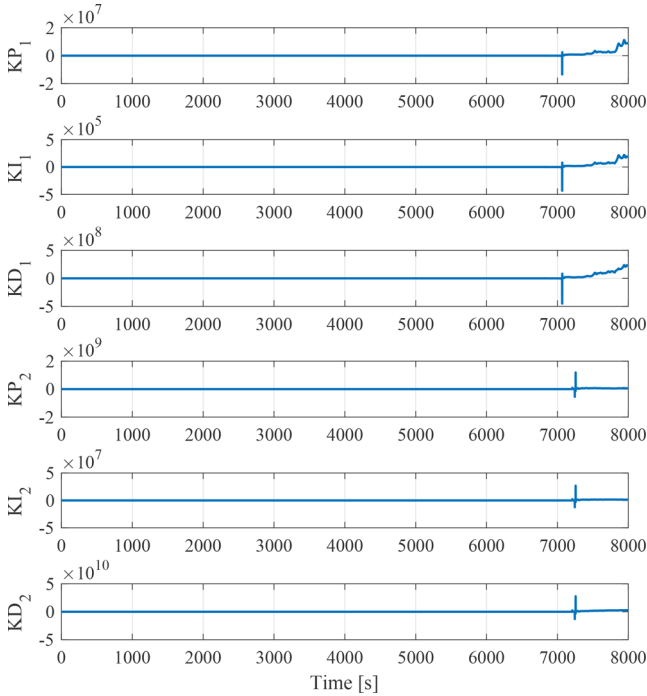


Figure 11. Trajectories of the PID gains corresponding to Figure 10.

0.05. Comparing the results shown in Figure 7 and Figure 12, oscillation of the inputs is reduced by using the GMVC-based controller. However, the output of the proposed method is more similar to the reference model than the result of the GMVC-based controller.

Time-Variant System. The previous section presented a result for a time-invariant system. In this section, a time-variant controlled object is considered because the proposed method is a self-tuning method. The following controlled object is considered:

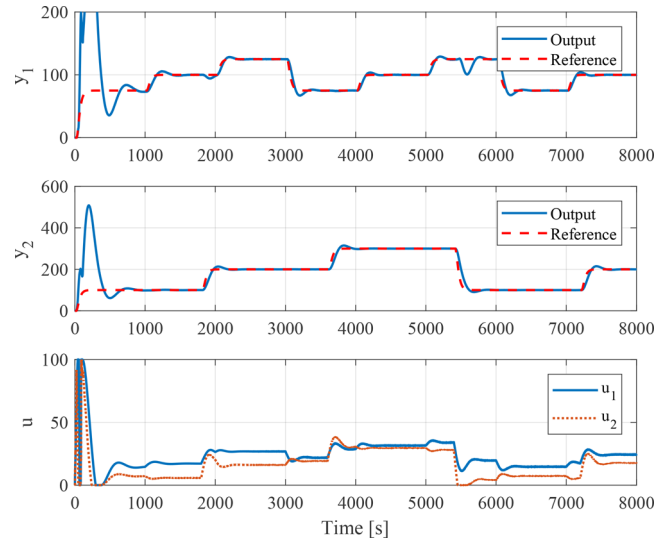


Figure 12. Control result for the time-invariant controlled object (eq 52) by using a multivariable self-tuning PID control method based on GMVC.

(i) $k < 3500$

$$\mathbf{G}(s) = \begin{bmatrix} \frac{7.3}{23s^2 + 83s + 1} e^{-25s} & \frac{-4.4}{14s^2 + 85s + 1} e^{-25s} \\ \frac{3.8}{19s^2 + 105s + 1} e^{-20s} & \frac{6.1}{18s^2 + 102s + 1} e^{-20s} \end{bmatrix} \quad (53)$$

(ii) $3500 \leq k$

$$\mathbf{G}(s) = \begin{bmatrix} \frac{5.11}{34.5s^2 + 124.5s + 1} e^{-25s} & \frac{-3.52}{22.4s^2 + 136s + 1} e^{-25s} \\ \frac{4.56}{22.8s^2 + 126s + 1} e^{-20s} & \frac{7.93}{23.4s^2 + 132.6s + 1} e^{-20s} \end{bmatrix} \quad (54)$$

The system was discretized by $T_s = 1$ s and the following discrete-time system:

(i) $k < 3500$

$$\begin{bmatrix} y_1(k) \\ y_2(k) \end{bmatrix} = \begin{bmatrix} \frac{0.06z^{-1} + 0.02z^{-2}}{1 - 1.02z^{-1} + 0.03z^{-2}} z^{-25} & \frac{-0.04z^{-1} - 0.008z^{-2}}{1 - 0.99z^{-1} + 0.002z^{-2}} z^{-25} \\ \frac{0.03z^{-1} + 0.006z^{-2}}{1 - 0.995z^{-1} + 0.004z^{-2}} z^{-20} & \frac{0.05z^{-1} + 0.01z^{-2}}{1 - 0.99z^{-1} + 0.003z^{-2}} z^{-20} \end{bmatrix} \times \begin{bmatrix} u_1(k) \\ u_2(k) \end{bmatrix} + \begin{bmatrix} \xi_1(k) \\ \xi_2(k) \end{bmatrix} \quad (55)$$

(ii) $3500 \leq k$

$$\begin{bmatrix} y_1(k) \\ y_2(k) \end{bmatrix} = \begin{bmatrix} \frac{0.03z^{-1} + 0.01z^{-2}}{1 - 1.02z^{-1} + 0.03z^{-2}}z^{-25} & \frac{-0.02z^{-1} - 0.004z^{-2}}{1 - 0.995z^{-1} + 0.002z^{-2}}z^{-25} \\ \frac{0.03z^{-1} + 0.006z^{-2}}{1 - 0.996z^{-1} + 0.004z^{-2}}z^{-20} & \frac{0.05z^{-1} + 0.01z^{-2}}{1 - 0.996z^{-1} + 0.003z^{-2}}z^{-20} \end{bmatrix} \times \begin{bmatrix} u_1(k) \\ u_2(k) \end{bmatrix} + \begin{bmatrix} \xi_1(k) \\ \xi_2(k) \end{bmatrix} \quad (56)$$

where $\xi_i(k)$ denotes the Gaussian white noise sequence with zero mean and variance 0.01^2 . This system also has input saturation. The upper limit was set as 100 and the lower limit was set as 0.

Next, the control result of the proposed control scheme is shown as Figure 13. Furthermore, Figure 14 and Figure 15 show

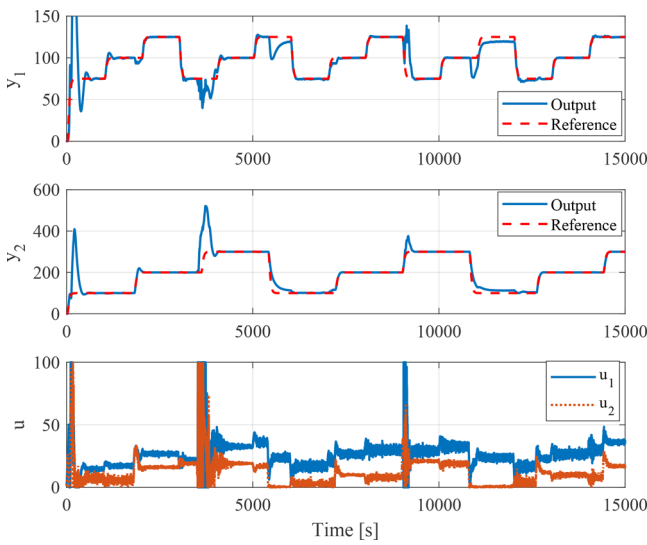


Figure 13. Control result for the time-variant controlled object (eq 56) by using the proposed control method.

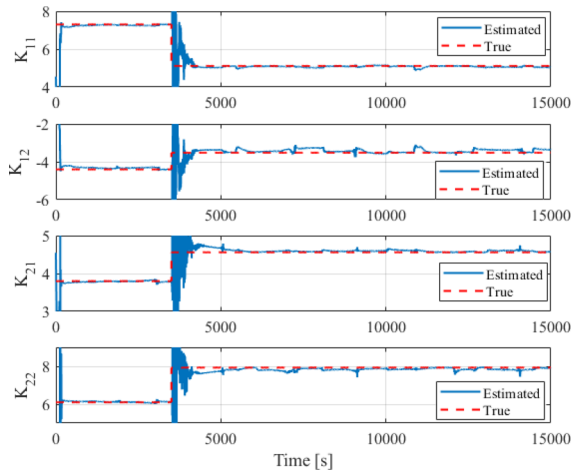


Figure 14. Trajectories of the system gain matrix corresponding to Figure 13.

the trajectories of the estimated system gains and PID gains, respectively. The user-specified parameters are set as shown in

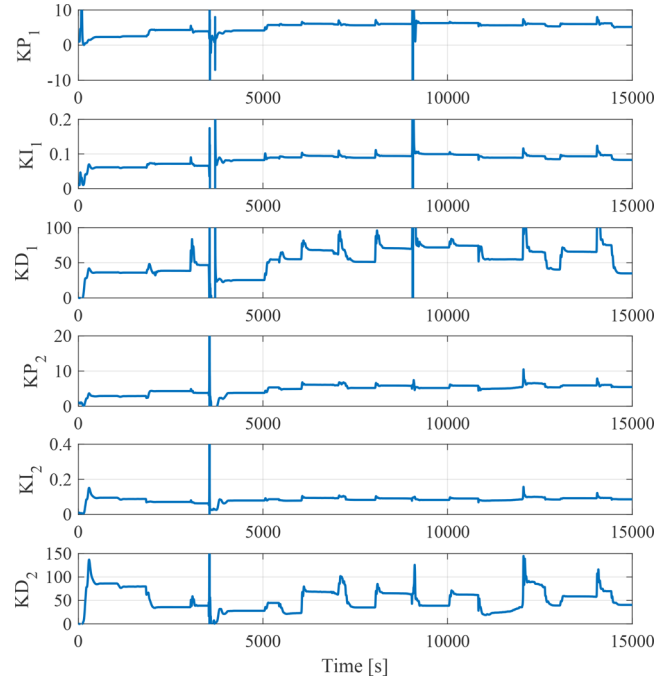


Figure 15. Trajectories of the PID gains corresponding to Figure 13.

Table 3. The proposed control method works well even if system parameters are varied. The estimated system gain matrix also converged to almost the same as the true values.

Table 3. User-Specified Parameters Corresponding to Figure 13

system parameters		PID gains	
n	10	σ_i	50
m	50	δ_i	0
d_p	0	d_i	known
$\omega_{1,i}$	0.995	$\omega_{2,i}$	0.995
$\alpha_{1,i}$	100	$\alpha_{2,i}$	100
c_1	0.95	c_2	0.5
$\hat{\theta}_{1,i}(0)$	unit vector	$\hat{\theta}_{2,i}(0)$	unit vector

EXPERIMENT

The previous sections presented numerical results. The results are obtained in an ideal condition. In this section, the proposed method is evaluated in an actual condition. A pilot-scale tank system is used to evaluate the proposed method. The system can be regarded as a first-order system with time delay. Figure 16 shows an appearance and schematic of the system. The control objective is to regulate the water level in the tank and the temperature of the mixed water simultaneously. There are two valves that manipulate the flow of the cold and hot water, respectively. The PID controller determines the position of the cold water's valve $u_c(k)$ and the hot water's valve $u_h(k)$ to regulate the level $y_1(k)$ and the temperature $y_2(k)$. In this section, the sampling time T_s is 5 s. $u_c(k)$ and $u_h(k)$ were associated with $y_1(k)$ and $y_2(k)$ as a main controlled input, respectively.

The control result using the proposed method is described below. The description is associated with the algorithm as mentioned in the simulation section. At first, the user-specified parameters were set as shown in Table 4. At the second to sixth steps, a decoupler was determined on the basis of the system

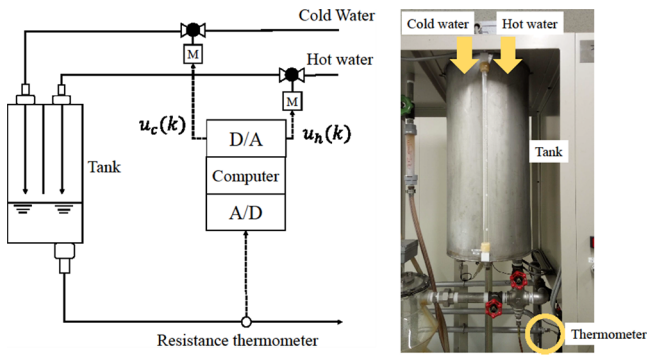


Figure 16. Appearance and schematic of the experimental tank system.

Table 4. User-Specified Parameters Corresponding to Figures 17 and 18

system parameters		PID gains	
n	10	σ_i	200
m	10	δ_i	0
d_p	0	d_1, d_2	5, 2
$\omega_{1,i}$	0.995	$\omega_{2,i}$	0.995
$\alpha_{1,i}$	100	$\alpha_{2,i}$	100
c_1	0.95	c_2	0.5
$\hat{\theta}_{1,i}(0)$	unit vector	$\hat{\theta}_{2,i}(0)$	unit vector

identification. In the experiment, a gain matrix between $u_c(k)$ and $u_h(k)$ to $y_1(k)$ and $y_t(k)$ was identified in every step, and a decoupler is also calculated on the basis of the gain matrix. At the seventh step, the output of the augmented output $\tilde{y}(k)$ was calculated by using the decoupler. At the eighth to 10th steps, PID gains were determined by a data-driven self-tuning PID scheme. When PID gains were determined, the input signals were $u_c(k)$ and $u_h(k)$, and the output signals were $\tilde{y}(k)$. At the 11th and 12th steps, the controlled inputs $u_c(k)$ and $u_h(k)$ were calculated.

The control result using the proposed method is shown in Figures 17 and 18. In addition, Figures 19 and 20 show the trajectories of the estimated system gains and PID gains, respectively. For these purpose of comparison, the control result without any decoupling decoupler is also shown in Figures 17

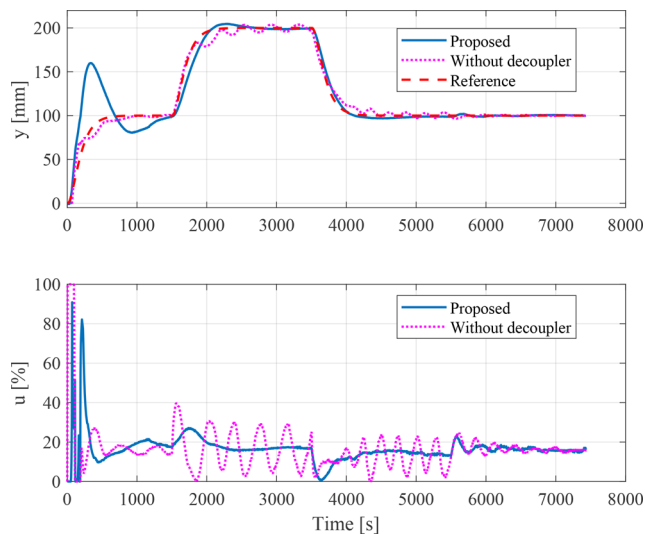


Figure 17. Experimental result of the level of water.

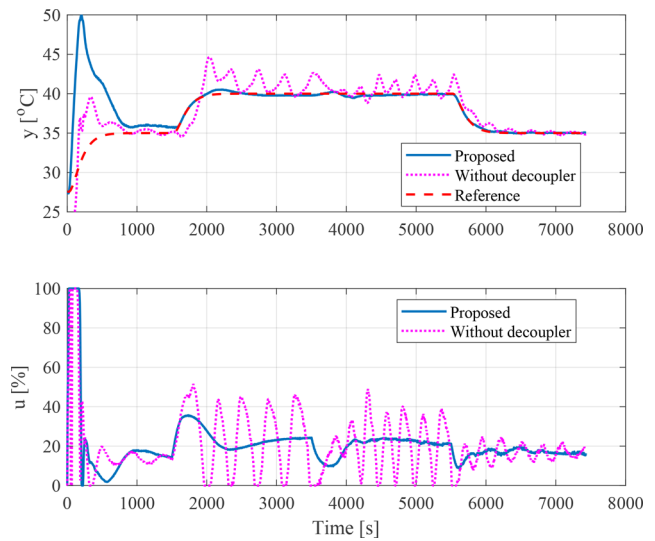


Figure 18. Experimental result of the temperature of water.

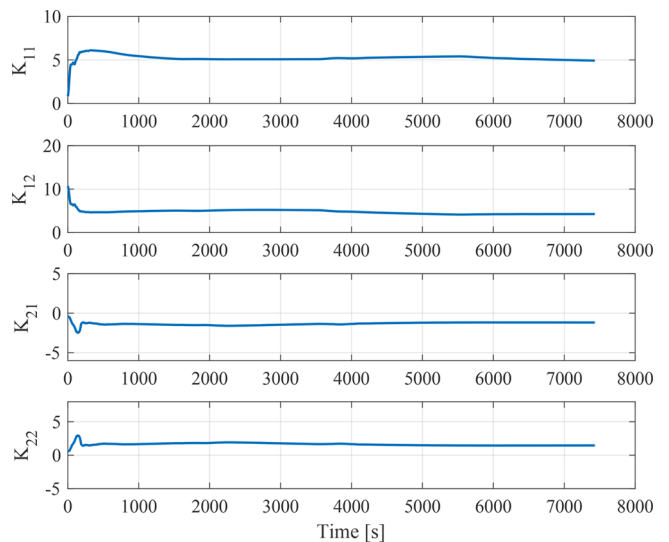


Figure 19. Trajectories of the system gain matrix corresponding to Figures 17 and 18.

and 18. By use of the proposed method, the system outputs were almost the same as the reference model outputs. In contrast, the system outputs were oscillatory without decoupler. Therefore, the proposed method is effective for the actual MIMO process.

CONCLUSIONS

In this paper, a design method of multiloop self-tuning PID control system has been proposed for a multi-input/multi-output system. The control scheme can be divided into two parts. One part is a decoupling part, and the static postdecoupler is employed in the proposed method. The other part is the designing multiloop PID controllers. These controllers have been newly designed by introducing the augmented output. The recursive least-squares algorithms are employed in both parts to determine the system gain matrix and PID gains. Features of the proposed control scheme are summarized as follows:

- A postdecoupler is introduced for the purpose of decoupling the controlled object, and the problem of the input saturation can be effectively avoided.
- The decoupler is based on a static system gain matrix.

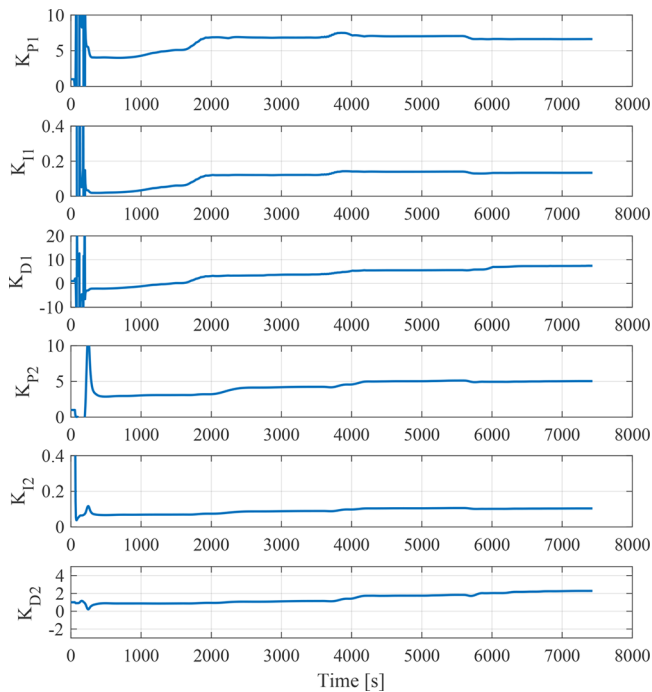


Figure 20. Trajectories of the PID gains corresponding to Figure 17 and 18

- Multiloop PID controller is designed on the basis of a minimization of the augmented error that derived from the PID control law.
- The static decoupler and PID gains are computed in an online manner.

Finally, the effectiveness of the proposed method have confirmed by some numerical examples and a pilot-scale tank system.

AUTHOR INFORMATION

Corresponding Author

*E-mail: yama@hiroshima-u.ac.jp. Phone: +81-82-424-7672. Fax: +81-82-424-7672.

ORCID

Toru Yamamoto: 0000-0001-6500-8394

Notes

The authors declare no competing financial interest.

ACKNOWLEDGMENTS

This work was supported by JSPS KAKENHI Grant Number JP16H04384.

REFERENCES

- (1) Soma, S.; Kaneko, O.; Fujii, T. A New Approach to Controller Parameter Tuning Based on One Experimental Data: A Proposal for Fictitious Reference Iterative Tuning. *J. Inst. Syst.* **2004**, *17*, 528–536.
- (2) Saeki, M. Direct Design of PID Controller Based on Transient Response Data. *IEEJ. Transactions on Electronics Information and Systems* **2011**, *131*, 722–725.
- (3) Dong, N.; Wu, C.-H.; Gao, Z.-K.; qiang Chen, Z.; Ip, W.-H. Data-driven control based on simultaneous perturbation stochastic approximation with adaptive weighted gradient estimation. *IET Control Theory and Applications* **2016**, *10*, 201–209.
- (4) Li, M.; Zhu, Y.; Yang, K.; Yang, L.; Hu, C.; Mu, H. Convergence Rate Oriented Iterative Feedback Tuning With Application to an

Ultraprecision Wafer Stage. *IEEE Transactions on Industrial Electronics* **2019**, *66*, 1993–2003.

(5) Åström, K. J., Hägglund, T., Eds. *Advanced PID Control*; International Society of Automation: Research Triangle Park, NC, 2005.

(6) Vilanova, R., Visioli, A., Eds. *PID Control in the Third Millennium*; Springer: Berlin, 2012.

(7) Desborough, L.; Miller, R. Increasing Customer Value of Industrial Control Performance Monitoring - Honeywell's Experience. *AIChE Symp. Ser.* **2002**, *98*, 169–189.

(8) Ashida, Y.; Hayashi, K.; Wakitani, S.; Yamamoto, T. A Novel Approach in Designing PID Controllers Using Closed-Loop Data. *Proc. American Control Conference* **2016**, 5308–5313.

(9) Ashida, Y.; Wakitani, S.; Yamamoto, T. Design of an Implicit Self-tuning PID Controller Based on the Generalized Output. *Proc. IFAC World Congress* **2017**, *50*, 13946–13951.

(10) Hayashi, K.; Yamamoto, T. Design of a Data Driven Multivariable PID Control System. *IEEJ. Transactions on Electronics Information and Systems* **2013**, *133*, 2229–2235.

(11) Yamamoto, T.; Shah, S. L. Design and experimental evaluation of a multivariable self-tuning PID controller. *IEE Proc.: Control Theory Appl.* **2004**, *151*, 645–652.

(12) Garrido, J.; Vazquez, F.; Morilla, F. Centralized multivariable control by simplified decoupling. *J. Process Control* **2012**, *22*, 1044–1062.

(13) Garrido, J.; Vazquez, F.; Morilla, F. An Extended Approach of Inverted Decoupling. *J. Process Control* **2011**, *21*, 55–68.

(14) Shigemasa, T.; Negishi, Y.; Baba, Y. Multivariable MD-PID control system design method and continuous system modeling. *Proc. Int. Symp. Adv. Control of Industrial Processes* **2014**, 85–89.

(15) Rosenbrock, H. H., MacFarlane, A. G. J., Eds. *StateSpace and Multivariable Theory*; Wiley Interscience: Hoboken, NJ, 1970.

(16) Katayama, M.; Yamamoto, T.; Mada, Y. A practical design of multiloop robust PID control systems. *IEE Proc. Control Theory and Applications* **2004**, *147*, 63–71.

(17) Formentin, S.; Savaresi, S. M.; Del Re, L. Non-iterative direct data-driven controller tuning for multivariable systems: theory and application. *IET Control Theory and Applications* **2012**, *6*, 1250–1257.

(18) Miskovic, L.; Karimi, A.; Bonvin, D.; Gevers, M. Correlation-based tuning of decoupling multivariable controllers. *Automatica* **2007**, *43*, 1481–1494.

(19) Garrido, J.; Vazquez, F.; Morilla, F. Multivariable PID control by inverted decoupling: Application to the Benchmark PID 2012. *Proc. IFAC Conf. Adv. PID Controllers* **2012**, *45*, 352.

(20) VanAntwerp, J. G.; Featherstone, A. P.; Braatz, R. D.; Ogunnaike, B. A. Cross-directional control of sheet and film processes. *Automatica* **2007**, *43*, 191–211.

(21) Precup, R.-E.; Tomescu, M. L.; Preitl, S.; Petriu, E. M.; Fodor, J.; Pozna, C. Stability analysis and design of a class of MIMO fuzzy control systems. *Journal of Intelligent and Fuzzy Systems* **2013**, *25*, 145–155.

(22) Pachauri, N.; Rani, A.; Singh, V. Bioreactor temperature control using modified fractional order IMC-PID for ethanol production. *Chem. Eng. Res. Des.* **2017**, *122*, 97–112.

(23) Vrkalovic, S.; Lunca, E.-C.; Borlea, I.-D. Model-Free Sliding Mode and Fuzzy Controllers for Reverse Osmosis Desalination Plants. *International Journal of Artificial Intelligence* **2018**, *16*, 208–222.

(24) Goodwin, G. C., Sin, K. S., Eds. *Adaptive Filtering Prediction and Control*; Prentice-Hall: Hoboken, NJ, 1984.